JOINT EUROPEAN TORUS

JET–P(91)23

P-H Rebut
and JET Team

Impact of JET Results on the Concept of a Fusion Reactor

"This document contains JET information in a form not yet suitable for publication. The report has been prepared primarily for discussion and information within the JET Project and the Associations. It must not be quoted in publications or in Abstract Journals. External distribution requires approval from the Publications Officer, JET Joint Undertaking, Abingdon, Oxon, OX14 3EA, UK".

"Enquiries about Copyright and reproduction should be addressed to the Publications Officer, EFDA, Culham Science Centre, Abingdon, Oxon, OX14 3DB, UK."

The contents of this preprint and all other JET EFDA Preprints and Conference Papers are available to view online free at www.iop.org/Jet. This site has full search facilities and e-mail alert options. The diagrams contained within the PDFs on this site are hyperlinked from the year 1996 onwards.

Impact of JET Results on the Concept of a Fusion Reactor

P-H Rebut
and JET Team*

JET-Joint Undertaking, Culham Science Centre, OX14 3DB, Abingdon, UK

** See Appendix 1*

Talk at AD Sakharov International Conference on Physics,
Moscow, USSR, 27-31 May 1991

Impact of JET Results on the Concept of a Fusion Reactor

P-H Rebut

JET Joint Undertaking, Abingdon, Oxon, OX14 3EA, UK

1. INTRODUCTION

Two approaches towards controlled thermonuclear fusion are being pursued at present - one based on inertial confinement and the other on magnetic confinement. A major step in the world programme would be the construction of the core of a first reactor. We are ready to take that step with the most advanced concept for magnetic confinement, namely the toroidal tokamak configuration. The tokamak originated in the USSR and JET is now the largest machine in operation.

The reactor will exploit the D-T reaction:

$$D + T \rightarrow {}^4He + n + 17.6MeV$$

The triple product of the temperature (T_i), density (n_i) and energy confinement time (τ_E) must exceed the value ($n_i.\tau_E.T_i$) of $5x10^{21}m^{-3}skeV$, typically with:

Central ion temperature, T_i	10-20keV
Central ion density, n_i	$2.5x10^{20}m^{-3}$
Global energy confinement time, τ_E	1 - 2s

During the early 1970's, it was clear that the achievement of near-reactor conditions required much larger experiments, which were likely to be beyond the resources of any individual country. In 1973, it was decided in Europe that a large device, the Joint European Torus (JET), should be built as a joint venture. The formal organization of the Project - the JET Joint Undertaking - was set up near Abingdon, UK, in 1978. The Project Team is drawn from Euratom and the fourteen member nations - the twelve EC countries, together with Switzerland and Sweden. By mid-1983, the construction of JET, its power supplies and buildings were completed on schedule and to budget and the research programme started.

JET is the largest project in the coordinated programme of EURATOM, whose fusion programme is designed to lead ultimately to the construction of an energy producing reactor. Its strategy is based on the sequential construction of major apparatus such as JET, the Next European Torus (NET), and DEMO (a demonstration reactor, which should be a full ignition, high power device), supported by medium sized specialized tokamaks.

The objective of JET is to obtain and study a plasma in conditions and dimensions approaching those needed in a thermonuclear reactor [1,2]. This involves four main areas:

(i) to study various methods of heating plasmas to the thermonuclear regime;

(ii) to study the scaling of plasma behaviour as parameters approach the reactor range;
(iii) to study the interaction of plasma with the vessel walls and how to continuously fuel and exhaust the plasma;
(iv) to study the production of alpha-particles generated in the fusion of deuterium and tritium atoms and the consequent heating of plasma by these alpha-particles.

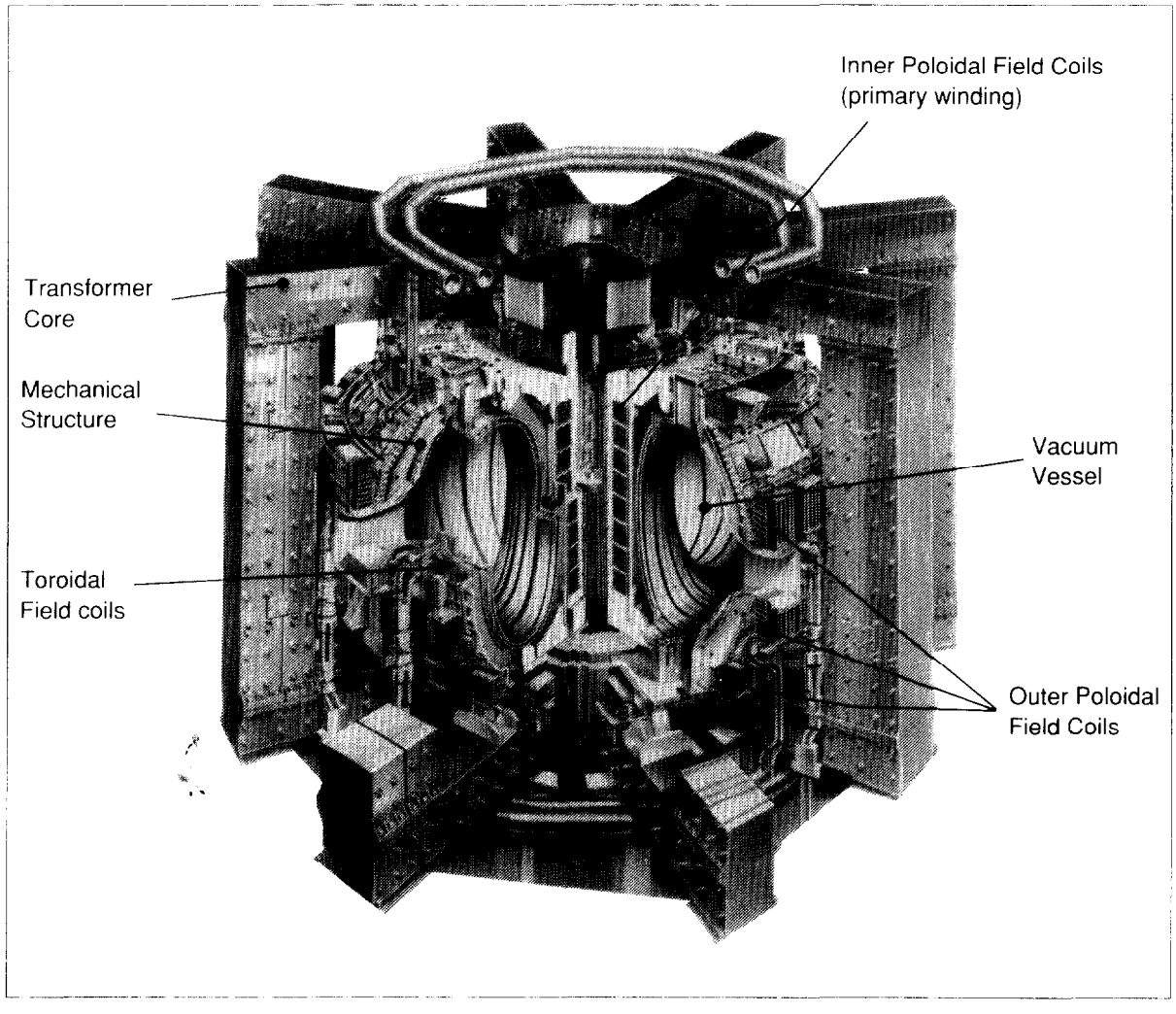

Fig. 1: The JET tokamak

To date, JET (see Fig.1) has successfully achieved and contained plasmas of thermonuclear grade, and has reached near breakeven conditions in single discharges. These results have also allowed a clearer picture of energy and particle transport to emerge, resulting in the development of the critical electron temperature gradient model, which describes and predicts the behaviour of plasmas.

Furthermore, a moderate extrapolation of latest results and considerations of model predictions, taken together with the constraints of present technology, allow the size and performance of a thermonuclear reactor to be largely defined. Most critical for a reactor is the control of impurities and the exhaust of helium ash at high power. To consolidate the model and provide

further information on density and impurity control, a New Phase is planned for JET with an axisymmetric pumped divertor configuration to operate with a stationary plasma (10-60s) of thermonuclear grade. A Next Step device must bridge the gap from present knowledge to that required to construct a first reactor.

This paper starts in Section 2 by setting out the basic elements of the tokamak configuration as a containment system, and describes the JET tokamak as a specific example. Sections 3 and 4 of the paper set out the main results achieved in JET. In Section 5, the critical electron temperature gradient model of plasma transport is formulated and applied to JET and a first reactor. In Section 6, the outstanding issues relevant to a reactor are discussed and, in particular, the question of impurity control and the New Phase of JET. In Section 7, a next step programme towards a fusion reactor is defined.

2. THE TOKAMAK AS A MAGNETIC CONTAINMENT SYSTEM

2.1 Basic Tokamak Configuration

The tokamak is the most advanced concept for containing magnetically a hot dense plasma [3]. A toroidal, axisymmetric plasma is confined by the combination of a large toroidal magnetic field, a smaller poloidal magnetic field (created by a toroidal current through the plasma) and the superposition of magnetic fields created by toroidal coils external to the plasma. The position and shape of the plasma cross-section is determined by the magnetic fields generated by these external coils.

The current circulating in the tokamak heats the plasma resistively. This Ohmic heating regime is limited to temperatures below ignition by the decrease in resistivity with increasing temperature, except, possibly, at the very highest densities and magnetic fields foreseen today. Auxiliary heating is required to reach higher temperatures. This can be in the form of the injection of beams of high energy neutral particles (NB); electromagnetic waves in different frequency ranges such as ion cyclotron resonance heating (ICRH), lower hybrid heating (LHH), etc. In an ignited D-T plasma, collisional heating due to the thermalization of energetic alpha-particles will be dominant.

The effectiveness of the heating in achieving the desired temperatures is determined largely by the thermal insulation of the plasma and is measured by the global energy confinement time, τ_E. Unfortunately, energy confinement is worse than would be expected on the basis of kinetic theory with binary collisions between particles (the so-called neo-classical theory) and a theoretical model for the anomalously poor insulation is needed. Empirical scaling laws for the energy confinement time have been derived on the basis of statistical fits to experimental data. The scalings which characterize discharges with additional heating (the low confinement or L-regime) are quite different from, and more pessimistic than, those for Ohmic heating alone. However, the expectations of L-regime scalings have been exceeded by up to a factor of about three in some regimes of plasma operation, the most notable of which is the H-regime (or high confinement regime).

The plasma density can be increased by: the injection of cold gas, high energy neutral particles and frozen solid pellets. Since the central plasma apparently shows better confinement than the overall plasma, central fuelling is highly desirable.

The environment of the plasma and the system chosen to define the plasma edge and to

exhaust particles and energy is also important. The first-wall that the plasma encounters can be a copious source of impurities to cool and poison the hot plasma. Therefore a careful choice must be made of the material used, as this determines the extent of this impurity problem. One option is a material limiter, in which a solid structure is introduced to define the plasma boundary (see Fig.2). An alternative is a poloidal magnetic divertor (X-point magnetic configuration), in which the plasma boundary is defined by the transition between closed, nested magnetic surfaces and the open magnetic field lines, which eventually intersect target plates away from the main plasma. A divertor can be considered as a limiter, remote from the plasma.

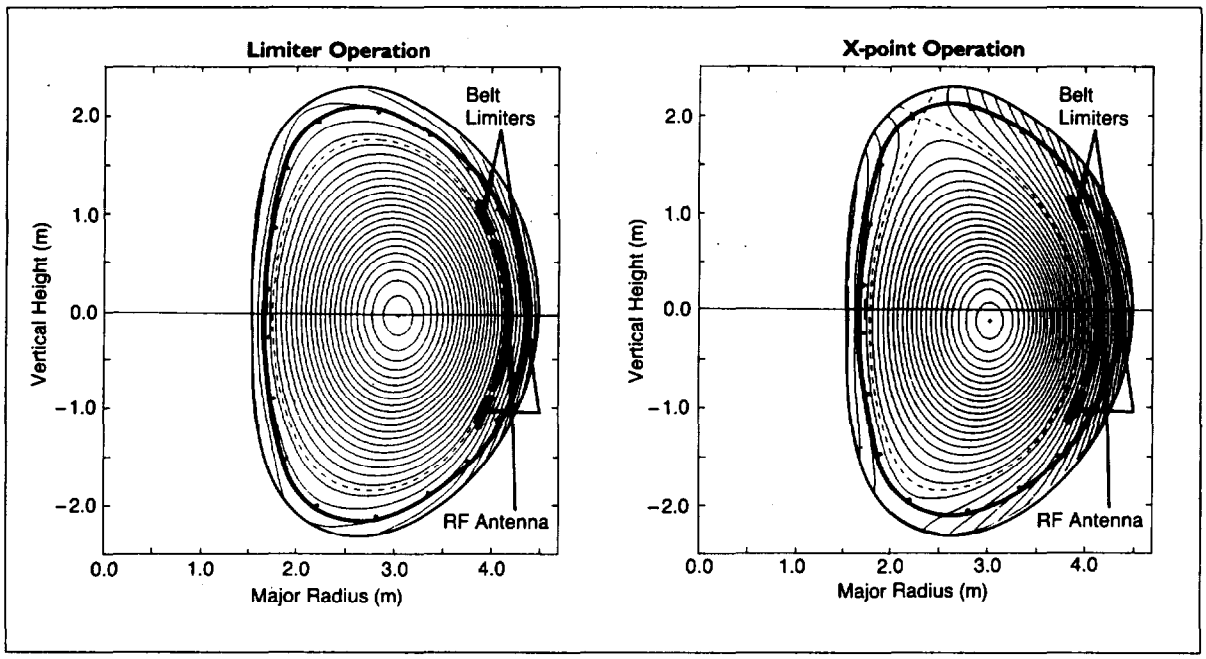

Fig. 2: The material limiter and the magnetic divertor (X-point) configurations

Table I: JET Parameters

Parameter	Design Values	Achieved Values
Plasma Major Radius (R_O)	2.96m	2.5 - 3.4m
Plasma Minor Radius (Hor)(a)	1.25m	0.8 - 1.2m
Plasma Minor Radius (Vert)(b)	2.1m	0.8 - 2.1m
Toroidal Field at R_O	3.45T	3.45T
Plasma Current	4.8MA	7.0MA
Neutral Beam Power	20MW	21MW
ICRF Heating Power	15MW	21MW

2.2 The JET Tokamak

JET is a high current, high power tokamak with a low-Z first wall and elongated plasma [4,5], whose overall view is shown in Fig.1. It is now in the second half of its original experimental

programme. The technical design specifications of JET have been achieved in all parameters and exceeded in several cases (see Table I). Furthermore, JET operates with the configuration foreseen for a Next Step tokamak. The plasma current of 7MA in the limiter configuration [6] and the current duration of up to 30s at 3MA are world records and are over twice the values achieved in any other fusion experiment. 5.1MA and 4.5MA are also the highest currents achieved in the single-null and double-null magnetic divertor configurations, respectively [7]. Neutral beam injection (NBI) heating has been brought up to full power (~21MW) and ion cyclotron resonance heating (ICRH) power has also been increased to ~21MW in the plasma. In combination, these systems have delivered 36MW to the plasma. The overall fusion triple product as a function of central ion temperature is shown in Fig. 3 for JET and a number of other tokamaks.

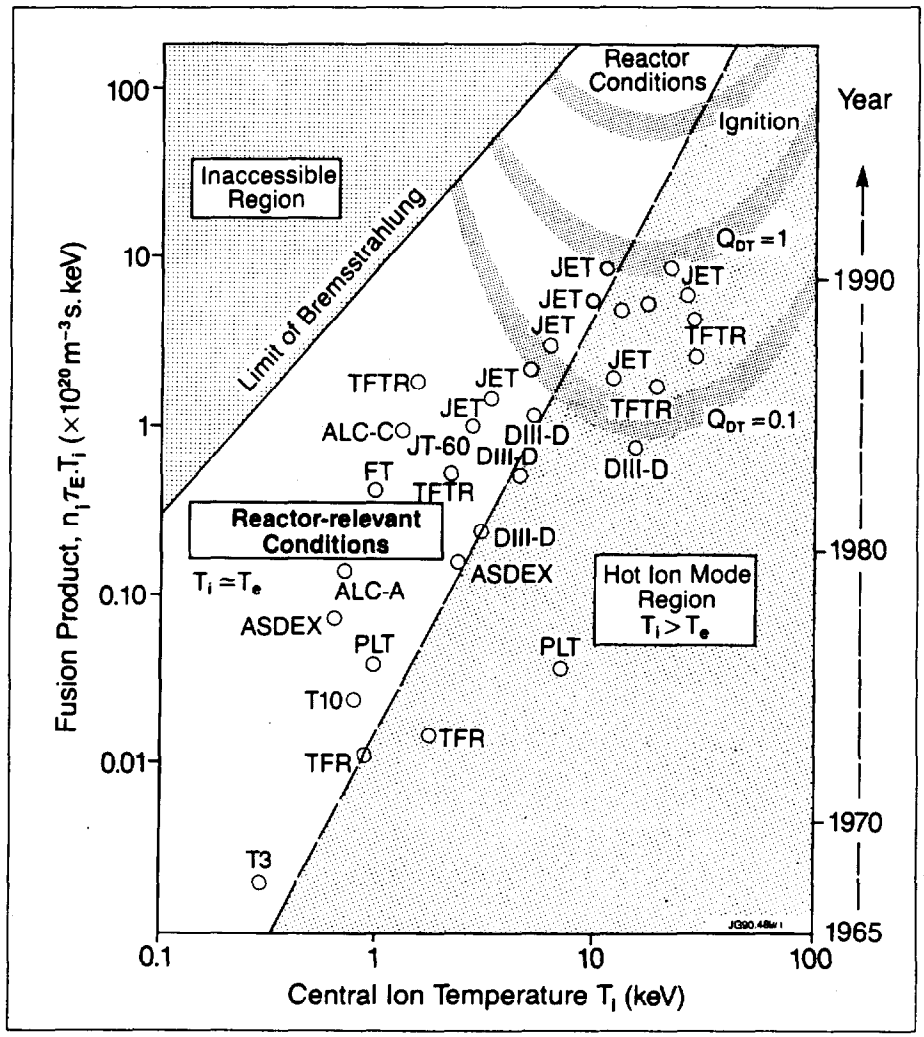

Fig. 3: Overall performance of the fusion product ($n_D \tau_E T_i$) as a function of central ion temperature (T_i), for a number of tokamaks

JET can operate with a magnetic limiter configuration (X-point configuration) and the regime of higher energy confinement (H-mode) has been observed in this configuration. The energy confinement time is then about twice the normal (L-mode) values. In both regimes, confinement degradation occurs in that the plasma thermal energy does not increase in proportion to the heating power. Therefore, considerably more power is needed to increase the plasma tempera-

ture and energy. In these experiments, impurities in the plasma at high power levels became a problem to further enhancing plasma parameters.

3. JET PERFORMANCE RELEVANT TO A DEMO

3.1 Use of Beryllium in JET

Recently, impurities and density control have been the main obstacles to the improvement of JET performance. Carbon first-wall components had been developed so that they were mechanically able to withstand the power loads encountered. However, the interaction of the plasma with these components, even under quiescent conditions, caused unacceptable dilution of the plasma fuel. In addition, imperfections in the positioning of the components led to localised heating at high power, and the following problems occurred:

- the production of impurities increased with the input power to the plasma;
- at high power, the heat load on the tiles caused a plasma evolution which exhibited a catastrophic behaviour - the so-called "carbon catastrophe". Increased plasma dilution, increased power radiated, reduced neutral beam penetration and a threefold fall of fusion yield resulted from the carbon influx;
- for lower input power with long duration, problems were also encountered. Without fuelling, deuterium was pumped by the carbon and replaced by impurities, resulting in severe dilution of the plasma.

The situation has been redressed by the progressive introduction of beryllium "first-wall" components since 1989 [8]. First, beryllium was evaporated as a thin layer on the carbon walls and limiters; then, as the material for the limiter tiles; and finally, as the material for the lower X-point target tiles and the open screens of the ICRH antennae.

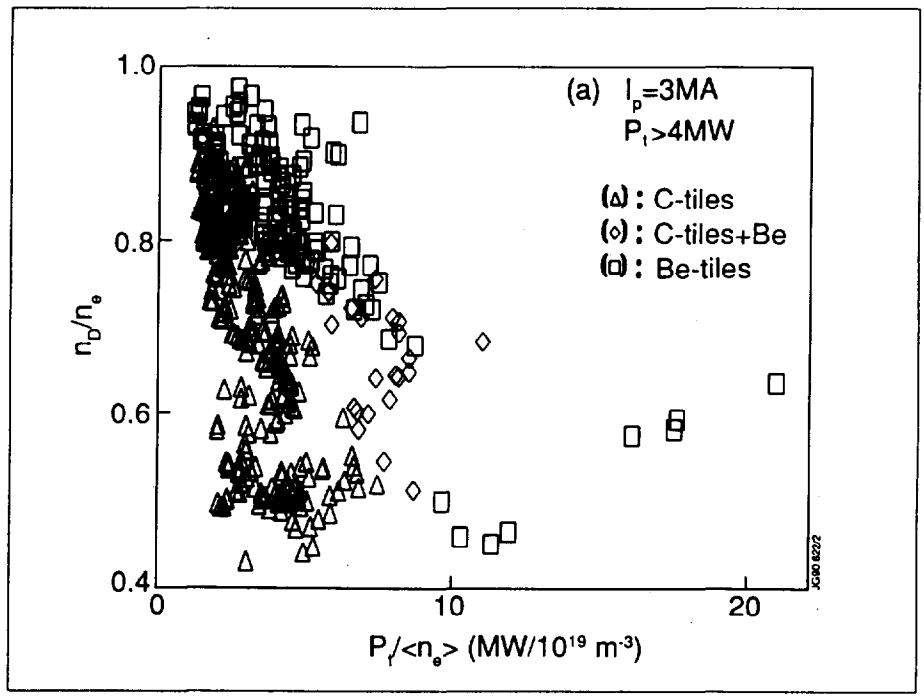

Fig. 4: The dilution factor, n_D/n_e, as a function of input power per particle, $P/<n_e>$

With a carbon first-wall, the main impurities were carbon (2-10%) and oxygen (1-2%). With beryllium evaporated inside the vessel, oxygen was reduced by factors >20, and carbon by >2. Although beryllium increased, carbon remained the dominant impurity for this phase. With beryllium limiters, the carbon concentration was reduced by a further factor of 10, but beryllium levels increased by ~10, and became the dominant impurity. Due to the virtual elimination of oxygen and replacement of carbon by beryllium, impurity influxes were reduced significantly, in line with model calculations [9] which take account of impurity self-sputtering. In addition, nickel was eliminated from the plasma when the nickel screens for the ICRH antennas were replaced by beryllium.

During 1989, plasma dilution and the effective plasma charge, Z_{eff}, were reduced significantly in ohmic plasmas and with strong additional heating. Fig. 4 shows the dilution factor, n_D/n_e, as a function of input power per particle, $P_t/\langle n_e \rangle$. With moderate power, it was not possible to maintain n_D/n_e much above 0.6 with carbon, but values greater than 0.8 were routinely achieved with beryllium. Furthermore, high power operation was possible only with beryllium.

Impurity radiation was also reduced and operation with beryllium gettering allowed improved density control (due to high wall pumping of both deuterium and helium). On the longer timescale (minutes to hours), very little deuterium was retained compared with a carbon first-wall; >80% of the neutral gas admitted to JET is recovered, compared with ~50% with a carbon first-wall. This has important advantages for the tritium phase of JET operation.

3.2 Fusion Performance

Improved plasma purity was achieved in JET using beryllium as a first-wall material, by sweeping the X-point and by using strong gas-puffing in the divertor region. This resulted in high ion temperatures (the hot-ion mode with T_i in the range 20-30keV) and improved plasma performance, with the fusion triple product ($n_D.\tau_E.T_i$) increasing significantly. Such improved fusion performance could otherwise have been achieved only with a substantial increase in energy confinement.

In the hot-ion H-mode regime, the central ion temperature reached 22keV, the energy confinement time, τ_E, was 1.1s, with a record fusion triple product ($n_D.\tau_E.T_i$) of $9\times10^{20}m^{-3}skeV$. The neutron yield for this discharge was also amongst the highest achieved on JET at 3.8×10^{16} ns^{-1}. A simulation of the pulse, assuming that the experiment had been performed in a D-T mixture, showed that 12MW of fusion power would have been obtained transiently with 16MW of NBI power. This would have reached near breakeven conditions and been within a factor of 8 of that required for a reactor. Similar results with ICRH were also obtained at medium temperatures, with $T_e \sim T_i \sim 10keV$.

However, the best fusion performance was obtained only **transiently** (for one confinement time (~1s)) and could not be sustained in steady state. Ultimately, the influx of impurities caused a degradation in plasma parameters. In fact, density and impurity control have been the main obstacles limiting JET performance.

4. QUANTITATIVE UNDERSTANDING OF FUSION PLASMAS

The underlying JET results are presented with particular emphasis on their significance for the formulation of a model of transient and steady state plasmas that can be used for moderate extrapolation to a Next Step tokamak.

4.1 Density Limit

The maximum attainable density in a tokamak is often limited by the occurrence of disruptions (or disruptive instabilities) and a complete loss of thermal insulation. With a beryllium first-wall, the maximum operating density increased significantly by a factor 1.6 - 2 compared with a carbon first-wall. Furthermore, the nature of the density limit changed and the frequency of disruptions at the density limit was much reduced. Disruptions did not usually occur, and the limit was associated rather with the formation of a poloidally asymmetric, but toroidally symmetric structure (a "MARFE"), in which radiation and atomic processes are dominant and which limit the operating domain for plasma density.

Heating and plasma fuelling were varied systematically, using both gas and pellet fuelling. With deep pellet fuelling and either NBI or ICRH, peaked profiles were obtained (Fig. 5). Just before a density limit MARFE occurred, pellet fuelled discharges reached the same edge density as gas fuelled discharges, but the central densities were considerably higher. The central density depends, therefore, on the fuelling method used. The profiles are similar near the edge, but are remarkably flat with gas fuelling.

These observations suggest that the edge density may be correlated with the density limit and is found to increase approximately as the square root of power [10] (see Fig. 6). This endorses the view that the density limit is determined by a power balance at the plasma edge and the cause of disruptions is related to radiation and charge exchange there. Thus, where beryllium is the only impurity and when the radiation is low, and confined to the outermost edge, density limit disruptions are not observed.

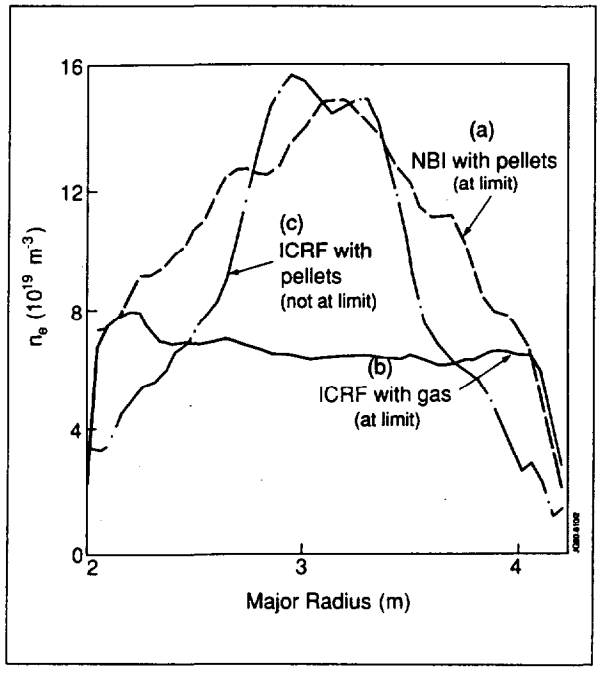

Fig. 5: Electron density profiles for different fuelling and heating methods. Profiles (a), (b) and (c) are correlated with their proximity to the density limit (see Fig.6)

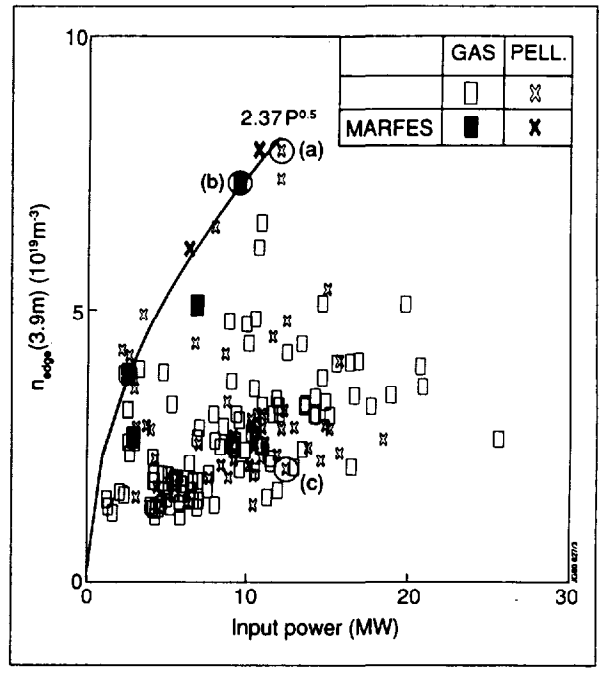

Fig. 6: The edge electron density (n_{edge}) versus input power (P) showing that the density limit occurs at the boundary of the operational domain close to the curve n_{edge} ($x10^{19}m^{-3}$) = 2.37 $P^{1/2}$(MW). The profiles in Fig.5 correspond to the three data points (a), (b) and (c).

4.2 Global Energy Confinement

The energy confinement time improves with increasing current and degrades with increasing heating power, independent of the heating method. With a carbon and beryllium first-wall, energy confinement times and their dependences are effectively identical: energy confinement does not appear to be affected by the impurity mix (carbon or beryllium in deuterium plasmas).

In the X-point configuration, high power H-modes (up to 25MW) have been studied. In comparison with limiter plasmas, confinement is a factor ~2 better, but the dependences with current and heating power are similar (Fig. 7). These observations are consistent with the same basic mechanism applying over most of the radius, except perhaps near the very edge.

4.3 Temperature

High ion temperatures have been obtained at the low densities possible with a beryllium first-wall and with the better penetration afforded by NBI at 140kV. Maximum ion temperatures were achieved of up to 22keV in limiter plasmas and up to 30keV in X-point plasmas (with powers up to 17MW). In this mode, the ion temperature profile is sharply peaked and the electron temperature is significantly lower than the ion temperature, by a factor of 2-3. The central ion temperature (as shown in Fig. 8) increases approximately linearly with power per particle up to the highest temperatures. Ion thermal losses are anomalous, but ion confinement degrades little with input power. On the other hand, the central electron temperature shows saturation at ~12keV, even though with ICRH the central heating power to the electrons appears to be higher than that to the ions. Electron thermal transport is anomalous and electron confinement degrades strongly with increased heating power. This suggests that electrons are primarily responsible for confinement degradation. However, this does mean that ion losses are necessarily small.

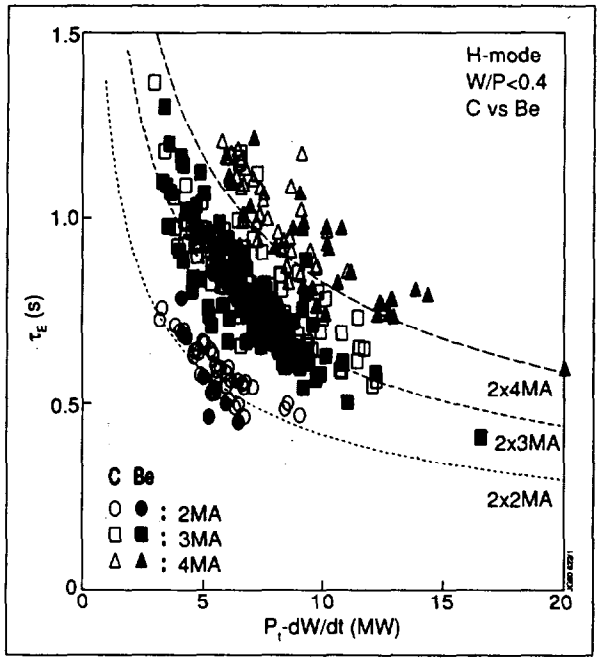

Fig. 7: Global energy confinement time (τ_E) during the H-mode as a function of net input power for different plasma currents and first wall materials

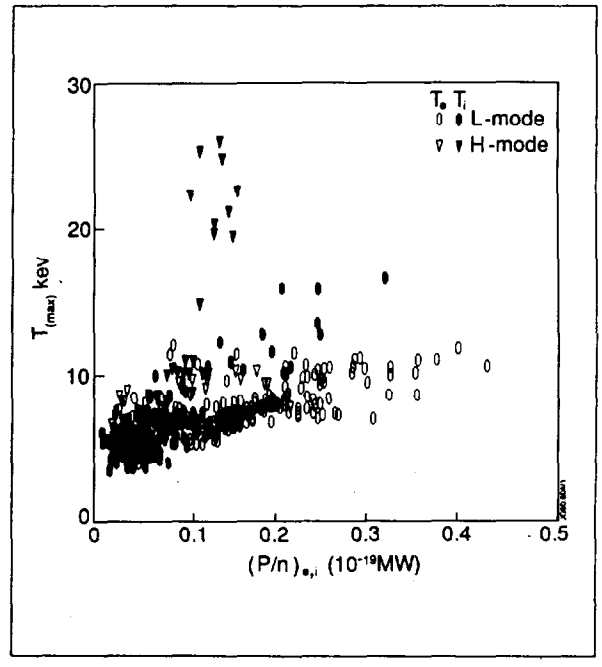

Fig. 8: Central ion (T_i) and electron (T_e) temperatures as functions of power per particle $(P/n)_{e,i}$ to either species

4.4 Electron Heat and Density Pulse Propagation

The propagation of temperature and density perturbations following a central temperature collapse (termed a sawtooth) provide good measurements of energy and particle transport. The decay of temperature perturbations in a 3MA/3.1T ohmically heated discharge is shown in Fig.9. This can be modelled with an heat pulse diffusivity, χ_{HP}~$3.2m^2s^{-1}$, compared with χ_e~$1m^2s^{-1}$, obtained from power balance considerations. The results in an L-mode plasma, heated with 9.5MW of ICRH, are also shown in Fig. 9 and indicate that, although χ_e~$2m^2s^{-1}$, the same χ_{HP}~$3.2m^2s^{-1}$ can be used in the simulation to fit the data. Within experimental uncertainties, the same χ_{HP} can be used also for H-regime plasmas and does not depend on heating power. Simultaneous measurements of the temperature and density perturbations indicate that the particle pulse diffusion coefficient, D_{PP}~D_e«χ_{HP} [11].

4.5 Plasma Pressure

Experiments indicate, and theory supports, the existence of a limit to the plasma pressure (indicated by the ratio of plasma and magnetic field pressures, the so-called β-value) that can be sustained in a tokamak. JET has explored the plasma behaviour near the expected β-limit in the double-null H-mode configuration, at high density and temperature and low magnetic field (B_t = 1T). β_t values up to ~5.5% were obtained, close to the Troyon limit $\beta_t(\%) = 2.8 I_p(MA)/B_t(T)a(m)$, where I_p is the plasma current and a is the plasma minor radius [10]. In JET, the limit does not appear to be disruptive at present power levels. Rather, a range of MHD instabilities occur, limiting the maximum β-value without causing a disruption.

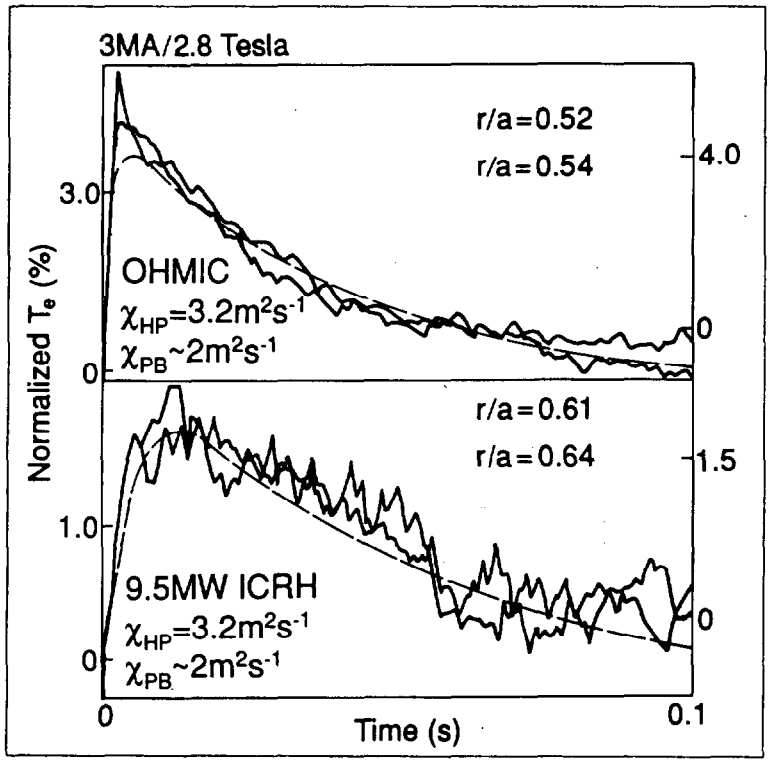

Fig. 9: Temporal evolution of electron temperature perturbations (normalised to the central electron temperature prior to collapse of a sawtooth) for 3MA/2.8T discharges with (a) ohmic heating only and (b) 9.5MW ICRH. Dashed lines are from model calculations using χ_{HP}=3.2m²s⁻¹

4.6 Alpha-particle Simulations

The behaviour of alpha-particles has been simulated in JET by studying energetic particles such as 1MeV tritons, and ^{3}He and H minority ions accelerated to a few MeV by ICRH [12]. Triton burn-up studies show that the experimental measurements of the 14MeV neutron rate is in good agreement with that calculated from the 2.5MeV neutron (and hence the 1MeV triton) source rate and classical thermalization. The energetic minority ion population with ICRH has up to 50% of the stored energy of the plasma and possesses all the characteristics of alpha-particles in an ignited plasma, except that in the JET experiments, the ratio of the perpendicular to parallel pressure was above three, while in a reactor plasma the distribution will be approximately isotropic. The mean energy of the minority species was about 1MeV, and the relative concentration of the ^{3}He ions to the electron density was 1-2%, which is comparable to the relative concentration of alpha-particles in a reactor (7%). Under conditions with little magneto-hydrodynamic (MHD) activity, no evidence of non-classical loss or deleterious behaviour of minority ions was observed, even though the ratio of fast ion slowing down time to energy confinement time in JET is greater than that expected in a reactor. The prospects for alpha-particle heating in DEMO should therefore be good. However, experiments do not address the possible loss of alpha-particles by the resonant interaction with Alfven modes.

5. A TRANSPORT MODEL

5.1 Formulation of a Plasma Model

Explaining the anomalous transport in tokamaks by the presence of turbulence is widely accepted. An analogy with turbulence in fluid mechanics can be developed [13]. The dimensionless Reynolds number, R, can be constructed from the physics quantities entering the Navier-Stokes equation and turbulence develops when R exceeds a critical value, R_c. Experimental data show that the laws ruling the flow change when the pressure gradient, i.e. the driving force, is such that $R>R_c$ (see Fig.10(a)).

Such a change in the energy and particle flows is also observed in a tokamak. Since the tokamak is an open thermodynamic system, heat flow could influence its stability. To conform with thermodynamics, the driving force for the heat transport in steady state should be the temperature gradient. The equivalent of the Reynolds number in fluid mechanics should be the ratio, $\nabla T/(\nabla T)_{cr}$ - a threshold value above which turbulence develops and the heat transport is enhanced. This behaviour is illustrated in Fig.10(b). With low power ohmic heating alone the temperature gradient should limit itself to a value close to, but above, the onset of turbulence. In the presence of powerful additional heating the confinement properties should be entirely controlled by the anomalous thermal transport.

It is certainly not unreasonable to assume that magnetic turbulence exists in a magnetic system[14]. In particular, macroscopic changes in the magnetic topology seems to be responsible for the total loss of confinement observed during major plasma disruptions. An attractive hypothesis is that a single basis, namely the magnetic topology, underlies the various phenomena observed in a tokamak, at least where atomic physics does not play a role. Tokamak physics would then be dominated by tearing and micro-tearing modes [15-20]. The topology would consist not only of well-nested magnetic surfaces but also of small magnetic islands surrounded by chaotic field lines connecting radially hot and cold regions [21]. Associated with

the magnetic topology, there will also be corresponding turbulence in the electric field and plasma density.

Experimental observations support a model for anomalous transport based on a single phenomenon and MHD limits. This **Critical Electron Temperature Gradient** model of anomalous heat and particle transport features:

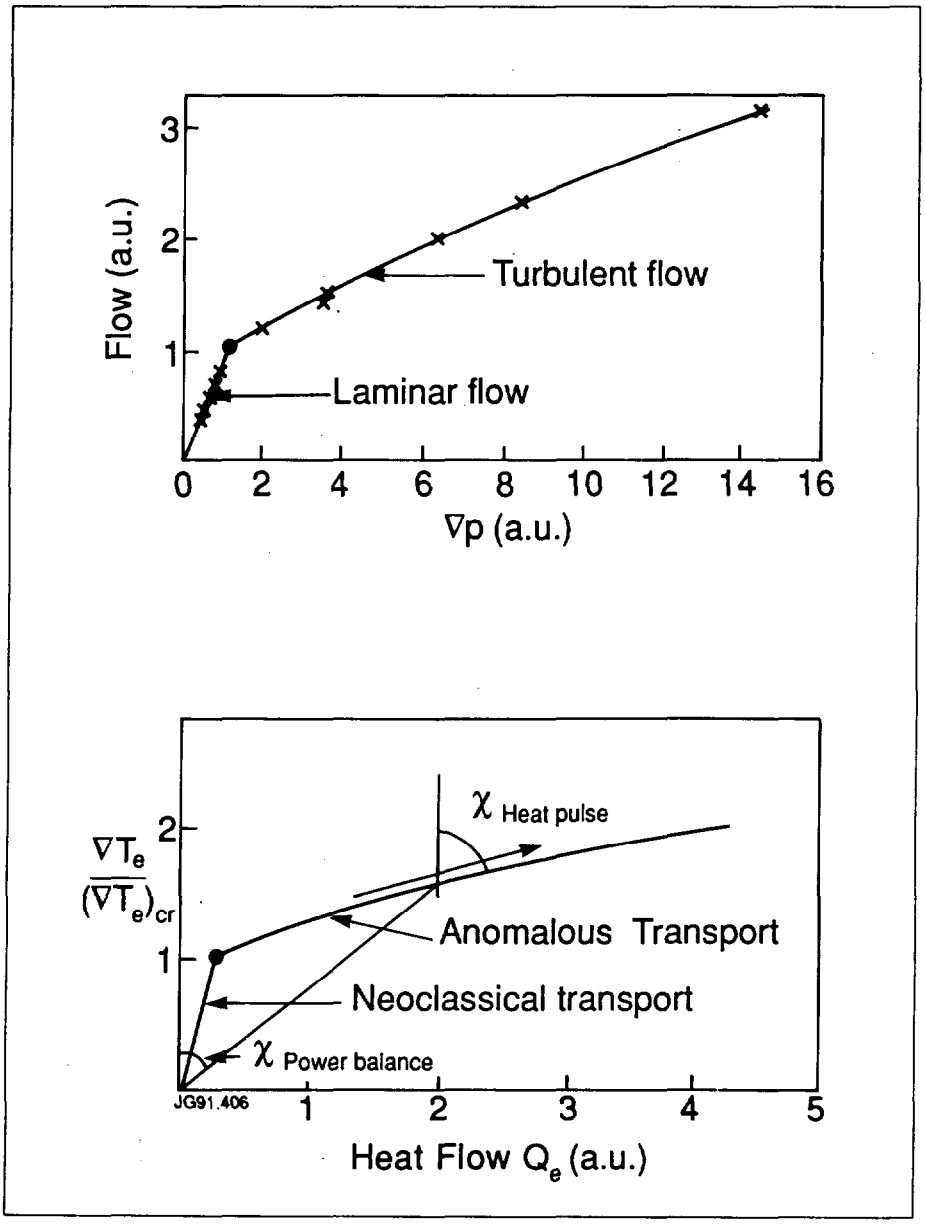

Fig. 10(a) the experimental relationship governing the flow of a liquid through a long pipe is shown. When the Reynolds number, R, reaches the critical value, R_c, extra resistance restricts the flow which increases with the value of R (curvature of the curve in the turbulent flow regime);

(b) for given temperature, density, magnetic field, etc., the dependence of the heat flow with electron temperature gradient in the critical temperature gradient model shows the same behaviour: when ∇T reaches $(\nabla T)_{cr}$, anomalous transport appears which increases the heat flow. This anomalous transport also varies non-linearly with the ratio $(\nabla T_e)/(\nabla T_e)_{cr}$.

- electrons which determine the degree of confinement degradation;
- ion anomalous transport with heat diffusivity χ_i linked to electron heat diffusivity χ_e;
- anomalous particle diffusivities, D, for ions and electrons, proportional to χ;
- anomalous inward particle convection for impurities alone.

Specifically, above a critical threshold, $(\nabla T_e)_{cr}$, in the electron temperature gradient, the transport is anomalous and greater than the underlying neoclassical transport. The electrons are primarily responsible for the anomalous transport, but ion heat and particle transport are also anomalous. The general expressions for the anomalous conductive heat fluxes are:

$$Q_e \equiv -n_e \chi_e \nabla T_e = -n_e \chi_{an,e} \left(\nabla T_e - (\nabla T_e)_{cr}\right) H(\nabla q)$$

$$Q_i \equiv -n_i \chi_i \nabla T_i$$

$$\chi_i = 2\chi_e \frac{Z_i}{\sqrt{1+Z_{eff}}} \sqrt{\frac{T_e}{T_i}}$$

$$D_\alpha = 0.7\chi_\alpha \qquad (\alpha \equiv \text{electrons, ions})$$

The critical electron temperature gradient model of Rebut et al [13] specifies possible dependences for $\chi_{an,e}$ and D and this has been explored further in subsequent work [4,5,22]:

$$\chi_{an,e} = 0.5c^2 \sqrt{\mu_0 m_i} \left(1 - \sqrt{\frac{r}{R}}\right) \sqrt{1+Z_{eff}} \left(\frac{\nabla T_e}{T_e} + 2\frac{\nabla n_e}{n_e}\right) \frac{q^2}{\nabla q} \frac{1}{B_T \sqrt{R}} \sqrt{\frac{T_e}{T_i}}$$

$$(\nabla kT_e)_{cr} = 0.06 \sqrt{\frac{e^2}{\mu_0 m_e^{1/2}}} \frac{1}{q} \sqrt{\frac{\eta j B_T^3}{n_e (kT_e)^{1/2}}}$$

This model features:

- a limitation in the electron temperature;
- electron heat pulse propagation with $\chi_{HP} \sim \chi_{an,e} > \chi_e$;
- no intrinsic degradation of ion confinement with ion heating power;
- density decay following pellet injection and its dependence on heating power;
- similar behaviour of particle and heat transport;
- particle pulse propagation, as observed with $D_{PP} \sim D_e \ll \chi_{HP}$.

Furthermore, in the plasma interior, the same model applies to the L- and H-regimes and particle and energy confinement improve together. However, at the edge of an H-regime plasma, an edge transport barrier forms and the transport might be classical over a short distance (~few cms). In fact, the H-regime may be the 'natural' consequence of the transport model, since $\chi_{an,e}$ depends on shear, and reduces towards zero near the separatrix. Furthermore, the reduction of MHD activity on making the transition from the L $\rightarrow$ H regime may imply the stabilisation of some other instability at the edge, where the effect of impurity radiation and neutral influxes on MHD might be important in destroying, at least partially, the edge confinement barrier. This instability is apparently easier to suppress in an X-point configuration with high edge magnetic or rotational shear.

5.2 Application of the Model to JET

The main predictions of the model are consistent with statistical scaling laws [13]. Furthermore, good quantitative agreement between the model and JET data has been established. As an example, the result of applying the model to the propagation of heat and density pulses following the collapse of a sawtooth in JET is shown in Fig. 11. The computed changes in T_e and n_e at various radii and times agree well with experiment.

The characteristics of an H-regime plasma can also be modelled, assuming classical transport near the separatrix. Fig. 12 shows that this leads to higher density and Z_{eff}, reduced edge flow (particle recycling simulated), higher stored energy and τ_E, lower χ_e and χ_i, as observed experimentally.

With such a model, we begin to have the predictive capability needed to define the parameters and operating conditions of a reactor, including impurity levels.

5.3 Definition of a First Reactor

A first reactor will be a full ignition, high power device (1-2GW electrical, 3-6GW thermal). This will include:

- auxiliary heating;
- D-T fuelling;
- divertor with high power handling and low erosion;

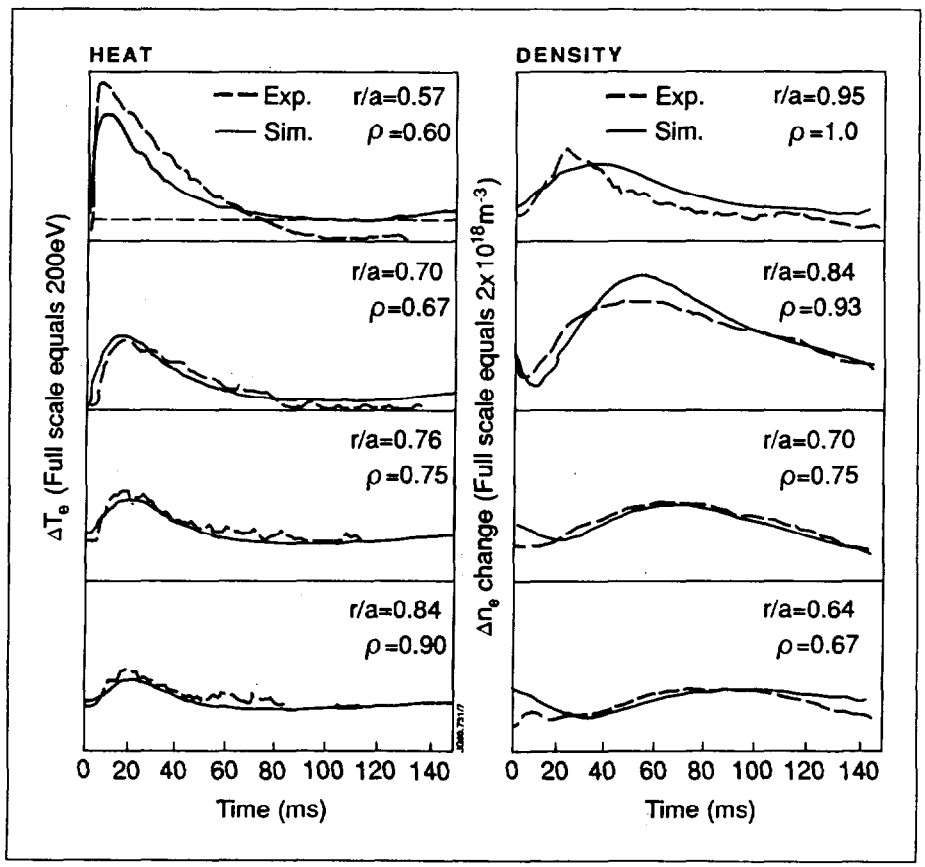

Fig. 11: Application of the model to the propagation of heat and density pulses following the collapse of a sawtooth in JET

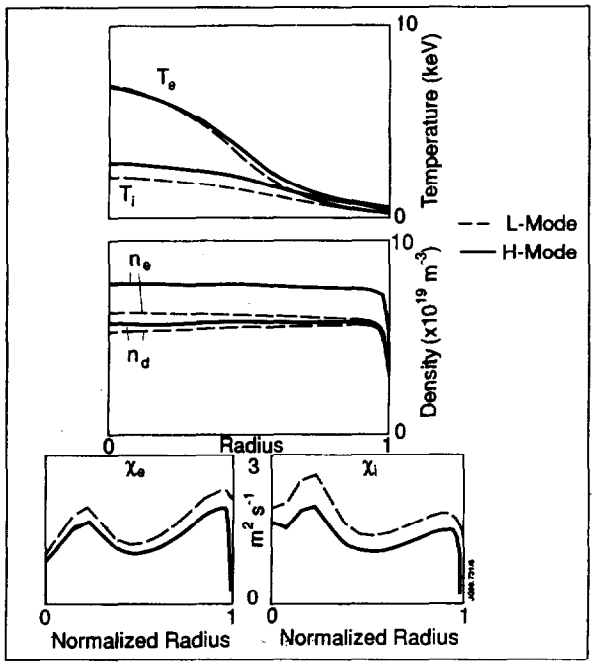

Fig. 12: The characteristics of an H-mode modelled, assuming classical transport near the separatrix

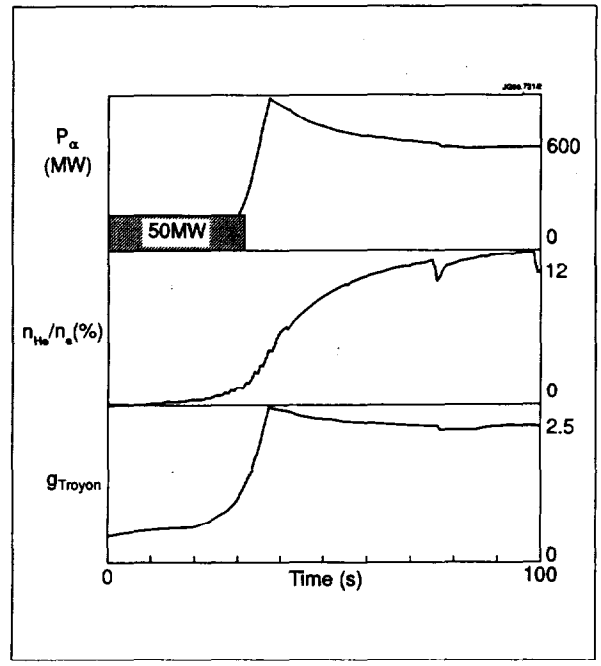

Fig. 13: Model of a first reactor plasma using the L-mode transport model tested against JET results

- exhaust for impurities and thermalized helium ash;
- first wall with high resilience to 14MeV neutrons;
- hot blanket to breed tritium;
- superconducting coils;
- plasma control.

The parameters of a first reactor are defined by technology and physics predictions. The minor radius of the reactor plasma needs to be twice the thickness of the tritium breeding blanket, which makes it ~3m and the elongation can be up to 2. A practical aspect ratio of ~2.5 sets the plasma major radius to 8m. Safe operation can be assumed for a cylindrical safety factor 1.6-1.8. Plasma physics requirements can be fulfilled by operating at a toroidal field no greater than 5T. This defines a reactor with a plasma current of ~30MA.

The operating conditions will be such that:

- $T_i \sim T_e$;
- confinement is L - mode;
- D-T mixture, including helium ash;
- sawteeth (minimum internal control from outside);
- high density, flat density profile;
- full impurity control.

5.4 Application of the Model to a First Reactor

We now model reactor plasmas using the L-mode transport model which has been tested against JET results, together with a model for sawteeth, β-limit instabilities and the divertor. A mixture of D-T is assumed and includes helium ash accumulation and pumping. Assuming the

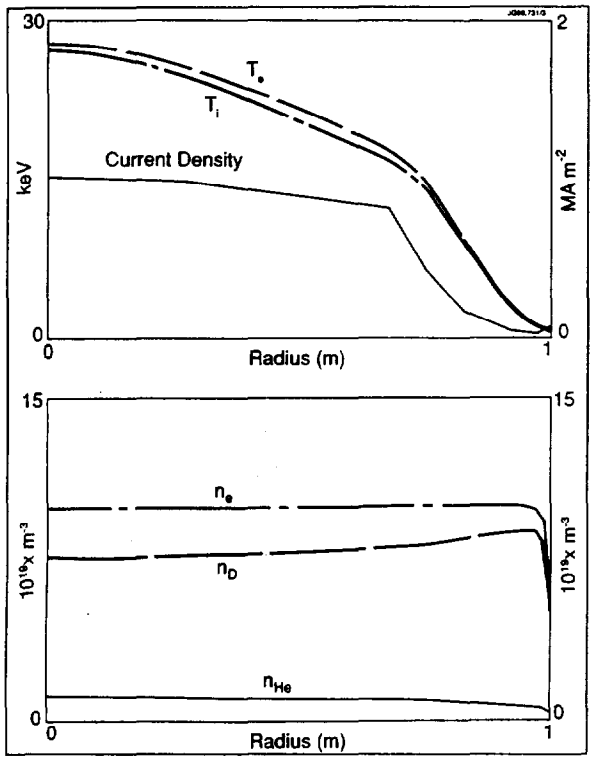

Fig. 14: DEMO profiles at ignition as a function of nomalized radius, ρ

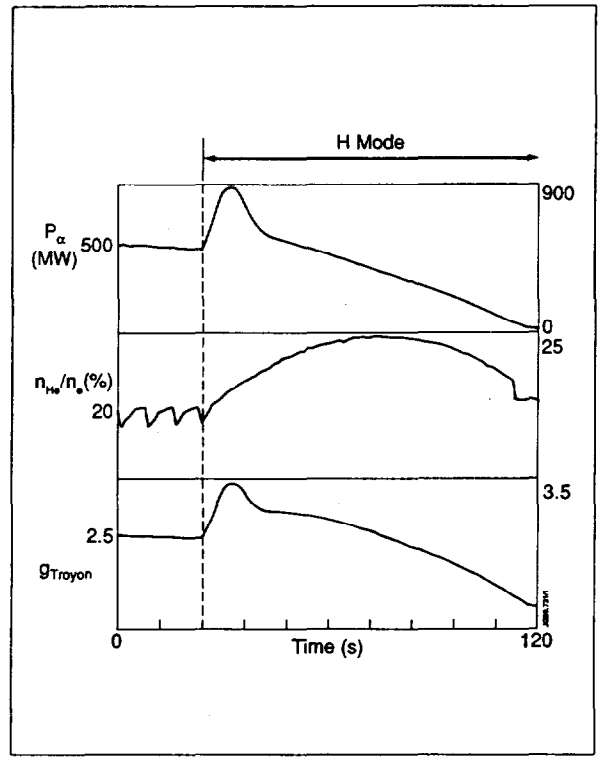

Fig. 15: Long term deficiencies due to helium poisoning in the H-mode

provision of adequate impurity control, ignition is maintained in the reactor (R=8m, a=3m, 4.5T, 30MA, κ=2) after switching off 50MW of ICRH (Fig. 13). At ignition, the slightly hollow density profiles (Fig. 14) with edge fuelling are sufficient to fuel the centre. However, helium poisoning alone can quench the ignition without adequate pumping. To exhaust sufficient helium and maintain ignition requires the pumping of about 1kg of D-T per hour. Exhaust and impurity control are essential. In fact, while the H-mode has short term benefits for approaching ignition, the long term deficiencies due to helium poisoning are evident (see Fig.15). Steady ignition conditions can be achieved with a specific level of helium ash.

With impurity control, ignition is achieved with edge fuelling and high pumping; high density and flat profile; sawteeth and L-mode confinement; and recirculation of a kg of D - T per hour. The H-mode does not improve steady state ignition due to the better confinement of helium ashes. At present, impurity control is envisaged to require high density operation. Under these conditions, the use of current drive seems precluded. However, one hour steady state requires only 50Vs (~10% of inductive Vs) and this can easily be provided.

6. SOLUTION OF OUTSTANDING ISSUES

6.1 Impurity Control in a Reactor

Plasma dilution is a major threat to a reactor and it is fundamental to bring dilution under control. There are two primary sources of dilution: target plate impurities and helium ash. A divertor concept for impurity control must be developed further. The fuelling, impurity control and exhaust capability of a Next Step will be dependent on whether deuterium and impurities

(including helium) accumulate in the plasma centre. The production and transport of helium ash towards the plasma edge (where it must be exhausted) will depend on the relative importance of energy and particle confinement, the effect of sawteeth, the effect of the edge transport barrier in the H-mode and the behaviour of the scrape-off layer plasma.

6.2 Impurity Control and the New Phase planned for JET

Active impurity control represents a solution to this problem, and will be tested in JET in a New Phase planned to start in 1992 [23]. First results should be available in 1993 and the Project should continue to the end of 1996.

The aim of the New Phase is to demonstrate, prior to the introduction of tritium, effective methods of impurity control in operating conditions close to those of a Next Step tokamak, with a stationary plasma of 'thermonuclear grade' in an axisymmetric pumped divertor configuration. Specifically, the New Phase should demonstrate:

- the control of impurities generated at the divertor target plates;
- a decrease of the heat load on the target plates;
- the control of plasma density;
- the exhaust capability;
- a realistic model of particle transport.

6.3 Key Concepts of the JET Pumped Divertor

Sputtering of impurities at the target plates presents a major difficulty and such impurities must be retained close to the target plates for effective impurity control. This retention may be accomplished by friction with a strong plasma flow directed along the divertor channel plasma towards the target plates [4,5,23-25]. The plasma flow will be generated by a combination of gas puffing, injection of low speed pellets and recirculation of a fraction of the flow at the target plates towards the X-point. The connection length along the magnetic field line between the X-point and the target plates must be sufficiently long to allow effective screening of impurities.

6.4 JET programme in the New Phase

The New Phase of JET should demonstrate a concept of impurity control; determine the size and geometry needed to realise this concept in a Next-Step tokamak; allow a choice of suitable plasma facing components; and demonstrate the operational domain for such a device.

A schedule for the JET programme incorporating the New Phase is shown in [4]. The earliest date to have a pumped divertor in JET is 1993. By the end of 1994, all information on particle transport, exhaust and fuelling, first wall requirements and enhanced confinement regimes needed to construct a Next Step tokamak, should be available. This concept could be developed further towards lower temperature, higher density, eg cold radiating plasma or gas target.

7. A PROGRAMME TOWARDS A FIRST REACTOR

The scientific feasibility of ignition under conditions required for a first reactor must first be demonstrated: that is, high power long pulse operation in a fully ignited plasma. Tritium breeding in hot blanket modules should also be tested. Advanced divertors and concept development aimed at improved efficiency must also be pursued.

Technology must still emerge on such items as pumping and helium extraction; the use of low-

Z plasma facing materials (eg. beryllium, carbon, carbides); the nature of breeding materials and coolant and structural materials for tritium breeding blankets. The resistance of highly sensitive materials (eg insulators, first-wall, etc.) to high neutron fluences should be evaluated. Industrial development is also required for superconducting coils which can withstand neutrons and AC losses. It is expected that the remaining technology can be scaled up from existing knowledge.

Many of these issues are expected to mature on differing timescales. A tokamak addressing all these issues would be close to a first reactor. To incorporate all innovations that are likely to reach maturity at different times, several facilities are required with well targeted objectives.

International collaboration is the way to address the different Next Step issues. Several complementary facilities, each with separate, clearly defined objectives, would:

- reduce scientific and technological risks;
- allow flexibility to accommodate new concepts;
- allow cross-checking of results;
- be more practical in managerial and industrial terms;
- offer flexibility in location and time scheduling.

This programme towards a first reactor, with ITER (International Thermonuclear Experimental Reactor) being the first component, would ensure an efficient use of world resources.

In such an optimised Programme, the three main issues of long burn ignition, concept optimisation and materials testing would be separated and addressed in different facilities which would be constructed as technologies mature. The engineering design for each facility can be defined precisely, thereby allowing a high degree of confidence that objectives would be met. In support of this programme, 'National Programmes' comparable in size would be needed.

8. CONCLUSIONS

The following points have been made:

(a) JET is a successful example of international collaboration involving fourteen countries. This advanced tokamak exploits the most effective magnetic configuration developed so far and was constructed on time and to budget;

(b) JET has met all and even exceeded many of its design parameters and now operates in the configuration foreseen for a reactor;

(c) **Individually**, each of the plasma parameters n, T_i and τ_E required for a fusion reactor have been achieved in JET; **in single discharges**, the fusion product of these parameters has reached near break-even conditions and is within a factor 5 - 8 of that required in a fusion reactor;

(d) However, these good results were obtained only **transiently**, and were limited by impurity influxes due to local overheating of protection tiles;

(e) A quantitative understanding of fusion plasmas has improved with the development of a specific plasma model which agrees well with JET data;

(f) With such a model we begin to have a predictive capability to define the parameters and operating conditions of a reactor;

(g) Experimental results and model predictions suggest the importance of controlling impurities and helium ashes in a reactor;

(h) The divertor concept must be developed further to provide sufficient impurity control and exhaust;

(i) An effective international collaboration programme should comprise several facilities, with well-focussed objectives, starting with the construction of ITER.

With a concentration of world effort and a modest increase in resources, we can proceed with such a programme towards a reactor.

9. ACKNOWLEDGEMENTS

The author is indebted to Drs DJ Gambier, BE Keen and ML Watkins for assistance in preparation of the paper. In addition, he is grateful to the JET Team, without whom the results in this paper would not be available.

10. REFERENCES

[1] The JET Project - Design Proposal: EUR-JET-R5 (1976).

[2] P-H Rebut and BE Keen, Fusion Technology, **11**, (1987), 13.

[3] BB Kadomtsev, FS Troyon and ML Watkins, Nuclear Fusion, **30**, (1990), 1675.

[4] P-H Rebut and the JET Team, Plasma Physics and Controlled Nuclear Fusion Research, (Washington, DC, 1990), IAEA, Vienna, in press.

[5] P-H Rebut et al, Physics of Fluids, in press.

[6] PJ Lomas and the JET Team, Plasma Physics and Controlled Nuclear Fusion Research, (Washington, DC, 1990), IAEA, Vienna, in press.

[7] A Tanga and the JET Team, Plasma Physics and Controlled Nuclear Fusion Research, (Washington, DC, 1990), IAEA, Vienna, in press.

[8] PR Thomas and the JET Team, Plasma Physics and Controlled Nuclear Fusion Research, (Washington, DC, 1990), IAEA, Vienna, in press.

[9] DDR Summers et al., J. Nucl. Mat. **176** & **177**, (1990), 593.

[10] ACC Sips et al., Proc. of 16th Eur Conf. on Controlled Fusion and Plasma Physics (Venice, Italy, 1989)Vol. I, (1989), p.99.

[11] P Smeulders and the JET Team, Plasma Physics and Controlled Nuclear Fusion Research, (Washington, DC, 1990), IAEA, Vienna, in press.

[12] DFH Start and the JET Team, Plasma Physics and Controlled Nuclear Fusion Research, (Washington, DC, 1990), IAEA, Vienna, in press.

[13] P-H Rebut, PP Lallia and ML Watkins, Plasma Physics and Controlled Nuclear Fusion Research, (Nice, France, 1988) IAEA, Vienna, Nuclear Fusion Supplement, Vol 2, p.191.

[14] TH Stix, Nucl. Fusion, **18**, (1978), 3.

[15] HP Furth, et al., Phys. Fluids, **6**, (1963), 459.

[16] RD Hazeltine et al, Phys. Fluids, **18,** (1975), 1778.

[17] AB Rechester, MN Rosenbluth, Phys. Rev. Lett., **40,** (1978), 38.

[18] A Samain, Plasma Phys. Control. Fusion, **26,** (1984), 731.

[19] P-H Rebut, M Hugon, in Plasma Physics and Controlled Nuclear Fusion Research 1984 (Proc. 10th Int. Conf. London, 1984), Vol.2, IAEA, Vienna (1985), p.197.

[20] BB Kadomtsev, Comments Plasma Phys. Controll. Fus., **9,** (1985), 227.

[21] P-H Rebut, et al in Plasma Physics and Controlled Nuclear Fusion Research 1986 (Proc. 11th Int. Conf. Kyoto, 1986), Vol.2, IAEA, Vienna, (1987), p.187.

[22] A Taroni and the JET Team, Plasma Physics and Controlled Nuclear Fusion Research, (Washington, DC, 1990), IAEA, Vienna, in press.

[23] P-H Rebut, PP Lallia and BE Keen Proceedings of the 13th Symposium on Fusion Engineering, (IEEE, New York, USA, 1989),Vol.1, p.227.

[24] P-H Rebut, JET Contributions to the Workshop on the New Phase for JET: The Pumped Divertor Proposal (September, 1989), JET Report - JET R(89)16.

[25] M Keilhacker and the JET Team, Plasma Physics and Controlled Nuclear Fusion Research, (Washington, DC, 1990), IAEA, Vienna, in press.

APPENDIX 1.

THE JET TEAM

JET Joint Undertaking, Abingdon, Oxon, OX14 3EA, U.K.

J.M.Adams[1], F.Alladio[4], H.Altmann, R.J.Anderson, G.Appruzzese, W.Bailey, B.Balet, D.V.Bartlett, L.R.Baylor[24], K.Behringer, A.C.Bell, P.Bertoldi, E.Bertolini, V.Bhatnagar, R.J.Bickerton, A.Boileau[3], T.Bonicelli, S.J.Booth, G.Bosia, M.Botman, D.Boyd[31], H.Brelen, H.Brinkschulte, M.Brusati, T.Budd, M.Bures, T.Businaro[4], H.Buttgereit, D.Cacaut, C.Caldwell-Nichols, D.J.Campbell, P.Card, J.Carwardine, G.Celentano, P.Chabert[27], C.D.Challis, A.Cheetham, J.Christiansen, C.Christodoulopoulos, P.Chuilon, R.Claesen, S.Clement[30], J.P.Coad, P.Colestock[6], S.Conroy[13], M.Cooke, S.Cooper, J.G.Cordey, W.Core, S.Corti, A.E.Costley, G.Cottrell, M.Cox[7], P.Cripwell[13], F.Crisanti[4], D.Cross, H.de Blank[16], J.de Haas[16], L.de Kock, E.Deksnis, G.B.Denne, G.Deschamps, G.Devillars, K.J.Dietz, J.Dobbing, S.E.Dorling, P.G.Doyle, D.F.Düchs, H.Duquenoy, A.Edwards, J.Ehrenberg[14], T.Elevant[12], W.Engelhardt, S.K.Erents[7], L.G.Eriksonn[5], M.Evrard[2], H.Falter, D.Flory, M.Forrest[7], C.Froger, K.Fullard, M.Gadeberg[11], A.Galetsas, R.Galvao[8], A.Gibson, R.D.Gill, A.Gondhalekar, C.Gordon, G.Gorini, C.Gormezano, N.A.Gottardi, C.Gowers, B.J.Green, F.S.Griph, M.Gryzinski[26], R.Haange, G.Hammett[6], W.Han[9], C.J.Hancock, P.J.Harbour, N.C.Hawkes[7], P.Haynes[7], T.Hellsten, J.L.Hemmerich, R.Hemsworth, R.F.Herzog, K.Hirsch[14], J.Hoekzema, W.A.Houlberg[24], J.How, M.Huart, A.Hubbard, T.P.Hughes[32], M.Hugon, M.Huguet, J.Jacquinot, O.N.Jarvis, T.C.Jernigan[24], E.Joffrin, E.M.Jones, L.P.D.F.Jones, T.T.C.Jones, J.Källne, A.Kaye, B.E.Keen, M.Keilhacker, G.J.Kelly, A.Khare[15], S.Knowlton, A.Konstantellos, M.Kovanen[21], P.Kupschus, P.Lallia, J.R.Last, L.Lauro-Taroni, M.Laux[33], K.Lawson[7], E.Lazzaro, M.Lennholm, X.Litaudon, P.Lomas, M.Lorentz-Gottardi[2], C.Lowry, G.Magyar, D.Maisonnier, M.Malacarne, V.Marchese, P.Massmann, L.McCarthy[28], G.McCracken[7], P.Mendonca, P.Meriguet, P.Micozzi[4], S.F.Mills, P.Millward, S.L.Milora[24], A.Moissonnier, P.L.Mondino, D.Moreau[17], P.Morgan, H.Morsi[14], G.Murphy, M.F.Nave, M.Newman, L.Nickesson, P.Nielsen, P.Noll, W.Obert, D.O'Brien, J.O'Rourke, M.G.Pacco-Düchs, M.Pain, S.Papastergiou, D.Pasini[20], M.Paume[27], N.Peacock[7], D.Pearson[13], F.Pegoraro, M.Pick, S.Pitcher[7], J.Plancoulaine, J-P.Poffé, F.Porcelli, R.Prentice, T.Raimondi, J.Ramette[17], J.M.Rax[27], C.Raymond, P-H.Rebut, J.Removille, F.Rimini, D.Robinson[7], A.Rolfe, R.T.Ross, L.Rossi, G.Rupprecht[14], R.Rushton, P.Rutter, H.C.Sack, G.Sadler, N.Salmon[13], H.Salzmann[14], A.Santagiustina, D.Schissel[25], P.H.Schild, M.Schmid, G.Schmidt[6], R.L.Shaw, A.Sibley, R.Simonini, J.Sips[16], P.Smeulders, J.Snipes, S.Sommers, L.Sonnerup, K.Sonnenberg, M.Stamp, P.Stangeby[19], D.Start, C.A.Steed, D.Stork, P.E.Stott, T.E.Stringer, D.Stubberfield, T.Sugie[18], D.Summers, H.Summers[20], J.Taboda-Duarte[22], J.Tagle[30], H.Tamnen, A.Tanga, A.Taroni, C.Tebaldi[23], A.Tesini, P.R.Thomas, E.Thompson, K.Thomsen[11], P.Trevalion, M.Tschudin, B.Tubbing, K.Uchino[29], E.Usselmann, H.van der Beken, M.von Hellermann, T.Wade, C.Walker, B.A.Wallander, M.Walravens, K.Walter, D.Ward, M.L.Watkins, J.Wesson, D.H.Wheeler, J.Wilks, U.Willen[12], D.Wilson, T.Winkel, C.Woodward, M.Wykes, I.D.Young, L.Zannelli, M.Zarnstorff[6], D.Zasche[14], J.W.Zwart.

PERMANENT ADDRESS

1. UKAEA, Harwell, Oxon. UK.
2. EUR-EB Association, LPP-ERM/KMS, B-1040 Brussels, Belgium.
3. Institute National des Récherches Scientifique, Quebec, Canada.
4. ENEA-CENTRO Di Frascati, I-00044 Frascati, Roma, Italy.
5. Chalmers University of Technology, Göteborg, Sweden.
6. Princeton Plasma Physics Laboratory, New Jersey, USA.
7. UKAEA Culham Laboratory, Abingdon, Oxon. UK.
8. Plasma Physics Laboratory, Space Research Institute, Sao José dos Campos, Brazil.
9. Institute of Mathematics, University of Oxford, UK.
10. CRPP/EPFL, 21 Avenue des Bains, CH-1007 Lausanne, Switzerland.
11. Risø National Laboratory, DK-4000 Roskilde, Denmark.
12. Swedish Energy Research Commission, S-10072 Stockholm, Sweden.
13. Imperial College of Science and Technology, University of London, UK.
14. Max Planck Institut für Plasmaphysik, D-8046 Garching bei München, FRG.
15. Institute for Plasma Research, Gandhinagar Bhat Gujat, India.
16. FOM Instituut voor Plasmafysica, 3430 Be Nieuwegein, The Netherlands.
17. Commissiariat à L'Energie Atomique, F-92260 Fontenay-aux-Roses, France.
18. JAERI, Tokai Research Establishment, Tokai-Mura, Naka-Gun, Japan.
19. Institute for Aerospace Studies, University of Toronto, Downsview, Ontario, Canada.
20. University of Strathclyde, Glasgow, G4 ONG, U.K.
21. Nuclear Engineering Laboratory, Lapeenranta University, Finland.
22. JNICT, Lisboa, Portugal.
23. Department of Mathematics, Univeristy of Bologna, Italy.
24. Oak Ridge National Laboratory, Oak Ridge, Tenn., USA.
25. G.A. Technologies, San Diego, California, USA.
26. Institute for Nuclear Studies, Swierk, Poland.
27. Commissiariat à l'Energie Atomique, Cadarache, France.
28. School of Physical Sciences, Flinders University of South Australia, South Australia SO42.
29. Kyushi University, Kasagu Fukuoka, Japan.
30. Centro de Investigaciones Energeticas Medioambientales y Techalogicas, Spain.
31. University of Maryland, College Park, Maryland, USA.
32. University of Essex, Colchester, UK.
33. Akademie de Wissenschaften, Berlin, DDR.

CR 88.49.1A